Supplementary Information

Studying the active-site loop movement of the São Paolo Metallo-β-Lactamase-1

Jürgen Brem,‡[a] Weston B. Struwe,‡[b] Anna M. Rydzik,[a] Hanna Tarhonskaya,[a] Inga Pfeffer,[a] Emily Flashman,[a] Sander S. van Berkel,[a] James Spencer,[c] Timothy D.W. Claridge,[a] Michael A. McDonough,[a] Justin L.P. Benesch,*[b] and Christopher J. Schofield*[a]

[a] *Department of Chemistry, University of Oxford, 12 Mansfield Road, Oxford, OX1 3TA, United Kingdom; E-mail: christopher.schofield@chem.ox.ac.uk*

[b] *Department of Chemistry, Physical and Theoretical Chemistry Laboratory, University of Oxford, South Parks Road, Oxford, OX1 3QZ, United Kingdom; E-mail: justin.benesch@chem.ox.ac.uk*

[c] *School of Cellular and Molecular Medicine, University of Bristol, Medical Sciences Building, Bristol, BS8 1TD, United Kingdom*

‡These authors contribute equally to this work.

Contents:

General experimental

Materials. Chemicals were from Sigma-Aldrich or VWR.

di-Zn(II)-SPM-1 production. Recombinant di-Zn(II)-SPM-1 was produced as described.[1] Recombinant di-Zn(II)-SPM-1 was produced in *E. coli* BL21 (DE3) pLysS cells using 2TY medium supplemented with 50 μg/ml ampicillin and 34 μg/ml chloramphenicol. Cells were grown at 37 ºC for 2h 40 min, then the temperature was reduced to 30 ºC for 6h. Cells were harvested by centrifugation (10 min, 10g), then resuspended in 50 mL lysis buffer supplemented with DNAse, lysosyme and EDTA-free protease-inhibitors. The cells were then further lysed by sonication (2 x 7 min) and cell debris removed by centrifugation (23g, 30 min). The cell lysates were then loaded onto a 5 mL HisTrap HP column (GE Healthcare Life Sciences, Little Chalfont, UK), with 50 mM Tris pH 7.5, 500 mM NaCl, containing 20 mM imidazole, then eluted with an imidazole gradient (up to 500 mM imidazole). Fractions containing di-Zn(II)-SPM-1 were incubated overnight at 4 °C with 3C protease (1:100 w/w) and then purified using a 5 mL HisTrap HP column to give the untagged protein. The purity of the resulting fractions >90% (by SDS-PAGE) (see Figure S5). Fractions containing purified protein were concentrated by centrifugal ultrafiltration (10 kDa cutoff membrane). Concentrations of the purified proteins were determined using a ND-1000 NanoDrop spectrophotometer.

Protein MS. ESI -spectra were acquired in the positive ion mode using a Waters LCT Premier instrument equipped with a TOF analyser. An LCT Premier mass spectrometer (Waters) was coupled to an Agilent 1100 Series HPLC using a Chromolith® FastGradient RP-18 endcapped column equipped with a 50-2 HPLC column, made of monolithic silica (C_{18}, 2 x 50 mm, macropores with 1.6 μm diameter, *Merck*). The instrument was connected to a CTC-autosampler inlet system. A multi-step gradient over 10 min was run (solvent A 94.9% H_2O/5% CH_3CN/0.1% formic acid, solvent B 99.9% CH_3CN/0.1% formic acid; 0-1 min 5% B for equilibration, followed by a linear gradient to 100% B over 4 min, then 100% B for an additional 3 min, followed by a linear gradient over 2 min back to 5% B to re-equilibrate the column) to separate the protein samples at flow rates of 0.4 ml/min for the first 5 min and then 1.0 ml/min for the remaining time. The electrospray ionisation source used a capillary voltage of 3.2 kV and cone voltage of 25 V. Nitrogen was used as the nebulizer and desolvation gas at a flow rate of 600 l/h. Protein typically eluted as a peak between 3 and 5 min under these conditions. Calculated masses were obtained using the ExPasy ProtParam tool (http://web.expasy.org/protparam/).

Matrix-assisted laser desorption/ionization time of flight mass spectrometry (MALDI-ToF-MS) and MS/MS analyses were performed using a *Bruker Daltonics* Ultraflex™ MALDI-ToF/ToF machine, using flexControl™ 3.0 software. Spectra were recorded in the positive ion reflectron mode, typically with 32-38% laser energy. Calibration was performed on each day prior to the measurements using Peptide Calibration Standard II (*Bruker Daltonics*). Data were processed using *Bruker Daltonics* flexAnalysis™ 3.0 software and assigned manually. For MALDI measurements, 1 μL of the sample was mixed with 4 μL of 2,5-dihydroxybenzoic acid (DHB, 20 mg/mL in 50% CH_3CN/0.1% CF_3COOH) matrix and 2 μL of this sample-matrix mixture spotted onto a 24 x 16 MTP AnchorChip™ 384 T F MALDI target and allowed to air-dry before analysis.

Apo SPM-1 production. Apo SPM-1 was produced by EDTA treatment of the di-Zn(II)-SPM-1 (see above). The treated protein was further purified using a Superdex S200 column (300 mL) equilibrated with 20 mM Tris pH 7.5, 200 mM NaCl supplemented with 10 mM EDTA. Fractions containing purified protein were concentrated by centrifugal ultrafiltration (10 kDa cutoffs) and buffer exchanged to a Chelex 100 treated metal free buffer (50 mM HEPES, pH 7.5, 200 mM NaCl) using PD-10 columns. The purity of the resulting fractions was ascertained to be >90% by SDS-PAGE (see Figure S6). Concentrations of the purified proteins were determined using a ND-1000 NanoDrop spectrophotometer and the serial dilutions used in assays were calculated based on the original concentration.

Non-denaturing MS. A sample of the SPM-1 was desalted using a Bio-Spin column (Bio-Radm Hemel Hempsteadm U.K.) in 15 mM ammonium acetate (pH 7.5). The MS data were acquired using a Q-TOF mass spectrometer (Q-TOF micro, Micromass, Altrincham, U.K.) interfaced with a NanoMate (Advion Biosciences, Ithaca, NY) with a chip voltage of 1.7 kV and a delivery pressure 0.5 psi. The sample cone voltage was 50V with a source temperature of 100 ^oC. The pressure at the interface between the atmospheric source and the high vacuum region was fixed at 6.30 mbar. Data were processed with the MassLynx 4.0 (Waters).

Thermal shift assays on SPM-1. Assays were carried out in white 8 x 6 PCR wells; total assay volume per well: 50 μL with final concentrations of 2 μM protein and, where appropriate, 50 μM of added metal was used using $ZnCl_2$, $MnCl_2$ x $4H_2O$, $CoCl_2$ x $6H_2O$ or $NiCl_2$ x $6H_2O$ as the metal sources. A SYPRO Orange Protein Gel Stain stock solution in DMSO (5000x concentrate) was diluted 1:2500 in 50 mM HEPES or Tris buffer respectively, pH 7.5, containing 200 mM NaCl. Fluorescence readings (monitored at 492 nm excitation

and 610 nm emission) were taken in triplicate between 25 °C and 80 °C, increasing the temperature linearly in steps of 1°C every minute. Melting curves and the mean of triplicate experiments with error bars showing the standard error of the mean (±SEM) are depicted in Fig. S8.

SPM-1 crystallisation. Crystals of SPM-1 were grown using the sitting drop vapour diffusion method at 4 °C. Drops contained 1 μL of protein solution (27.8 mg/mL stock), combined with 1 μL of precipitant (0.05 M $MgCl_2$, 25-30 w/v jeffamine M-600, 0.15 M MES pH 6.5). Crystals were cryoprotected using well solution diluted with 25% glycerol before being flash cooled in liquid nitrogen. Data for SPM-1 were collected at 100K at Diamond Light Source synchrotron beamline I02. Data were indexed, integrated and scaled using HKL-3000.[2] The structure was solved by molecular replacement using PHASER[3] with the 'open' SPM-1 (PDB ID: 2FHX)[4] as a search model. The structure was then refined using PHENIX[5] and COOT[6] until R_{work} and R_{free} no longer converged. Data collection and refinement statistics are given in Table S2.

CCS measurements. A sample containing 10 μM of SPM-1 was desalted using a Bio-Spin column (Bio-Radm Hemel Hempsteadm U.K.) in 200 mM ammonium acetate (pH 7.4). CCS measurements were made using a modified Synapt G1 HDMS instrument (Waters Co., Manchester, UK) as previously described.[7] NanoESI measurements were performed using gold-coated borosilicate capillaries made in-house and instrument parameters were as follows: capillary voltage 1.4 kV, cone voltage 10 V, bias voltage 15 V, Helium pressure 1.36 Torr and the drift voltage was increased stepwise from 50 to 200 V. Theoretical CCS values were calculated using DriftScope v2.1 CCS Calculation software (Waters Co. Manchester, UK).

Mutagenesis

The Y152C SPM-1 variant was generated using the δ36 NDM-1 in the pOPINF plasmid as described.[1] The desired point mutation was achieved employing the QuikChange sites directed mutagenesis kit (Stratagene) using the following primers:

forward – 5'- TTCAGGTCTTCATTCTTGCAAAATTCGGCCGCTTTAATGC,

reverse – 5'- GCATTAAAGCGGCCGAATTTTGCAAGAATGAAGACCTGAA.

Expression trials were performed (see Fig S11), after lysis using the BugBuster kit (Merck Millipore)© (Note: the protein level correlates with enzyme activity as measured using a chromogenic substrate, nitrocefin). The SPM-1 Y152C variant was produced and purified using the same conditions as wild type SPM-1.

Y152C SPM-1 labelling. SPM-1 (Y152C) was labelled following the reported protocol for NDM-1* producing ^{19}F-labelled SPM-1 (SPM-1*).[8] Denaturing protein LC-MS confirmed the presence of uniformly mono-labelled protein after labelling (Fig. S13).

In-Solution Digestion Procedure. All reagents were prepared in 100 mM Tris buffer, pH 7.8. Samples (< 500 µg), then were dried in a Vacufuge® vacuum concentrator (*Eppendorf*) connected to an external diaphragm pump, and then resuspended in 100 µL of 6 M urea. Disulfides were reduced at room temperature (30 min) by addition of 5 µL of 200 mM dithiothreitol (DTT), and subsequently alkylated at room temperature (30 min) using 30 µL of 200 mM iodoacetamide. Unreacted alkylating reagent was consumed by addition of 30 µL DTT solution (30 min). The sample was then diluted with 775 µL Tris buffer, mixed with Sequencing Grade Modified Porcine Trypsin (*Promega*) at trypsin:protein sample ratio of ca. 1:50, and digested at 37 °C for 12h. Digestion was stopped by adjusting the sample to pH 3-4 by addition of concentrated acetic acid. Digested samples were subsequently purified and desalted by solid-phase extraction using Sep-Pak C_{18} Plus Light Cartridges (*Waters*, 130 mg sorbent per cartridge, 55-105 µM particle size) following the manufacturer's protocol. The samples were then dried using a Vacufuge® and subsequently re-dissolved in typically 15-30 µl of 50% CH_3CN/0.1% CF_3COOH for analysis by MALDI-ToF-MS.

^{19}F-NMR studies (kinetics). Kinetic and inhibition analyses were performed as described.[8] Samples contained the di-Zn(II)-SPM-1* complex (80 µM, unless otherwise stated) in Tris buffer (50 mM, pH 7.5) supplemented with 200 mM NaCl and 10% D_2O. CF_3COOH (TFA, 50 µM) was used as an internal standard (δ - 75.45 ppm). ^{19}F-NMR measurements were conducted using a Bruker AVII 500 or Bruker AVIII 600 spectrometer equipped with a 5mm z-gradient triple resonance inverse ^{1}H(^{13}C)/ ^{19}F TXI probe. ^{19}F{^{1}H} decoupled spectra were recorded at 298 K, using 5 mm diameter NMR tubes (Norell).

^{19}F-NMR studies (saturation transfer). NMR measurements were conducted using a Bruker AVII 500 spectrometer equipped with a 5mm z-gradient triple resonance inverse ^{1}H/^{19}F(13C) TXI probe operating at 298K using 5 mm diameter NMR tubes (Norell). Saturation transfer experiments were done using direct saturation on ^{19}F for 5 s with 63 mV power levels and saturation shifts -83.13, -72.3 or -90 ppm, respectively (as indicated in Table. S3). Exchange was demonstrated by exchange in the intensity of the signal (Table. S3). Spectra were recorded using 128 scans. Data were processed with 20 Hz Lorentzian line broadening using TopSpin 3.1 software (Bruker) and were referenced to the internal TFA standard (δ - 75.45 ppm). Samples contained SPM-1-2Zn(II) complex (300 μM) in Tris buffer (50 mM, pH 7.5) supplemented with 200 mM NaCl and 10% D_2O.

Magnetisation transfer experiments. NMR measurements were conducted using a Bruker AVII 600 spectrometer equipped with a 5mm z-gradient triple resonance inverse ^{1}H/^{19}F(13C) TXI probe operating at 298K using 5 mm diameter NMR tubes (Norell). Samples contained SPM-1-2Zn(II) complex (320 μM) in Tris buffer (50 mM, pH 7.5) supplemented with 200 mM NaCl and 10% D_2O.

The inversion was achieved with a hard pulse pair sequence prior to the variable delay (vd): ***90 – τ– 90 – vd – 90-Acquire.*** The transmitter frequency was placed on-resonance for one peak (-71.4 ppm) and with the delay τ set to 1/2ν where ν is the frequency separation (in Hz) between the two peaks (6208 Hz). This results in inversion of the on-resonance spin and return to the +z-axis of the off-resonance spin. Sixteen vd time points were used and 40 transients collected for each 1D spectrum using a recovery delay of 3s. Data were processed with 3 Hz line broadening using Bruker's TOPSPIN 3.2 software. Initial T_1 values were determined from a non-selective inversion recovery experiment (0.46 and 0.39 s for the -71.4 and -82.2 ppm peaks respectively) with data fitting performed using the Bruker TOPSPIN T1/T2 relaxation module. The resulting magnetisation exchange data are summarised in Table. S4. Data fitting was performed using the CIFIT routine.[9]

Zinc-dependence of SPM-1. Measurements were performed using 0.5 nM SPM-1 and 2.5 μM FC5.[1] Kinetic analyses were performed as previously described.[1] Note: an increasing rate of cephalosporin hydrolysis was observed with increasing zinc concentration in the assay buffer (see Fig. S22).

Stopped-flow reactions. Reactions were conducted at 5 °C and monitored using a using stopped-flow apparatus (Applied Photophysics, UK). Apo-SPM-1 was incubated for 10 min with different amounts of metal (Co(II), Zn(II)), and then rapidly mixed with nitrocefin in 1:1 ratio. The final concentrations were 50 uM SPM-1, 50 uM nitrocefin, 50/100/250 uM Co(II). The reaction was observed using a photodiode array detector and kinetic traces were analysed with KinTek Pro software.

Table S1. Outline properties of the different structural subclasses of MBLs.[10-16]

	B1	B2	B3
Gene Type	- Chromosomal and Plasmid	- Chromosomal	- Mainly Chromosomal, recent in plasmids
Metal coordination	- Zn1 site: HHH - Zn2 site: DCH	- Zn1 site: NHH (inhibitory) - Zn2 site: DCH	- Zn1 site: H(Q)HH - Zn2 site: DHH
Substrate specificity	- Broad spectrum	- Mainly carbapenems	- Penicillins and Cephalosporins
Characteristic active site loop(s)	- Flexible/hydrophobic L3 loop - hydrophilic L10 loop	- α3 loop[a] - hydrophilic L10 loop	- loop between α3 and strand β7

[a] Note L3 presents but lack of the extended mobile loop.

Figure S1. Sequence alignment of SPM-1 (B1 MBL, PDB ID: 2FHX), CphA (B2 MBL, PDB ID: 1X8I), Sfh-I (B2 MBL, PDB ID:3SD9), L1 (B3 MBL, PDB ID: 2FM6), NDM-1 (B1 MBL PDB ID:4EYF), VIM-2 (B1 MBL, PDB ID: 1KO2), IMP-1 (B1 MBL, PDB code: 1JJT) and BcII (B1 MBL, PDB ID:1BVT) MBLs. Note the 'insertion' of the α3 loop in the cases of CphA (B2), Sfh-I (B2) and SPM-1 (B1). (Sequences were obtained from the metallo-β-lactamase engineering database: http://www.mbled.uni-stuttgart.de/).

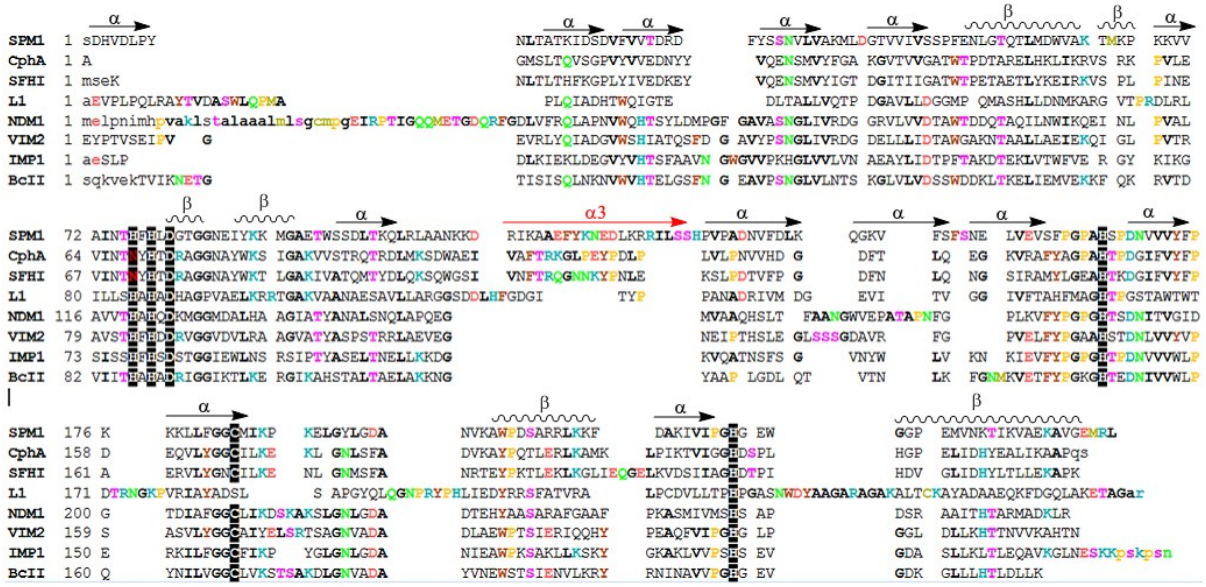

Figure S2. Views from MBL crystal structures. IMP-1 (B1 MBL, ID: 1JJT), CphA (B2 MBL, PDB ID: 1X8I), L1 (B3 MBL, PDB ID: 2FM6) and the 'open' and 'closed' form of SPM-1 (B1 MBL, 'open' PDB ID: 2FHX and 'closed' PDB ID: 4BP0) showing the conserved αβ/βα sandwich core fold of the MBLs. An elongated L3 loop is normally characteristic of the di-Zn(II) B1 MBLs. The mono-zinc B2 MBLs are characterised by an α3 region and a shorter L3 loop. In the case of the B1 MBLs only SPM-1 has the elongated α3 region and a short L3 loop.

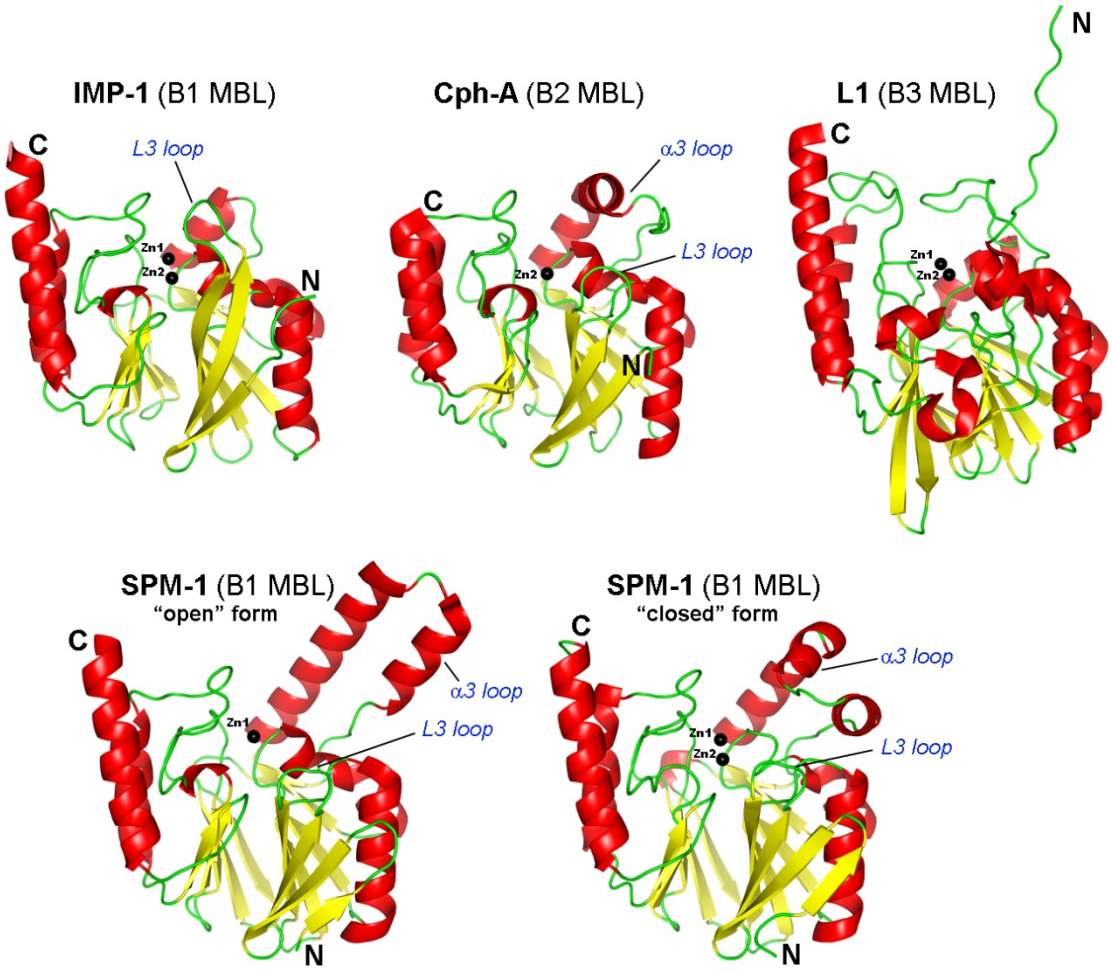

Figure S3. Surface representations of 'open' and 'closed' forms of SPM-1 (B1 MBL, 'open' PDB: 2FHX and 'closed' PDB: 4BP0) and 'closed' CphA, (B2, PDB code: 1X8I), Zn(II) atoms are shown as green spheres. Overall surfaces are shown in light gray, except for the α3 region show which is in dark gray.

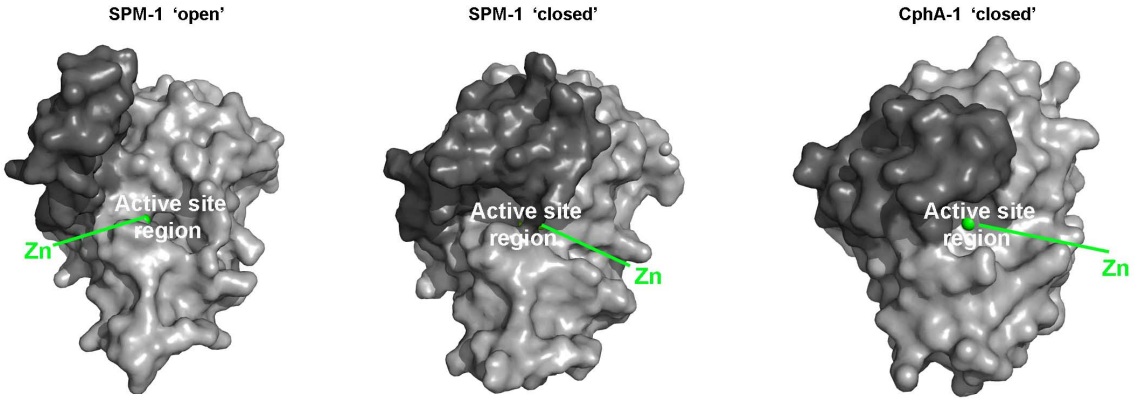

Figure. S4. Topologies of selected MBLs. Topology diagrams of IMP-1 (B1 MBL, PDB ID: 1JJT), CphA (B2 MBL, PDB ID: 1X8I) and SPM-1 (B1 MBL, 'open' PDB ID: 2FHX) showing the elongated L3 loop for IMP-1 (B1 MBL, residues 16-40) which is shorter for CphA (B2 MBL, residues 52-77) and SPM-1 (B1 MBL, residues 43-57) and the presence of the α3 loop for CphA (B2 MBL) and SPM-1 (B1 MBL).

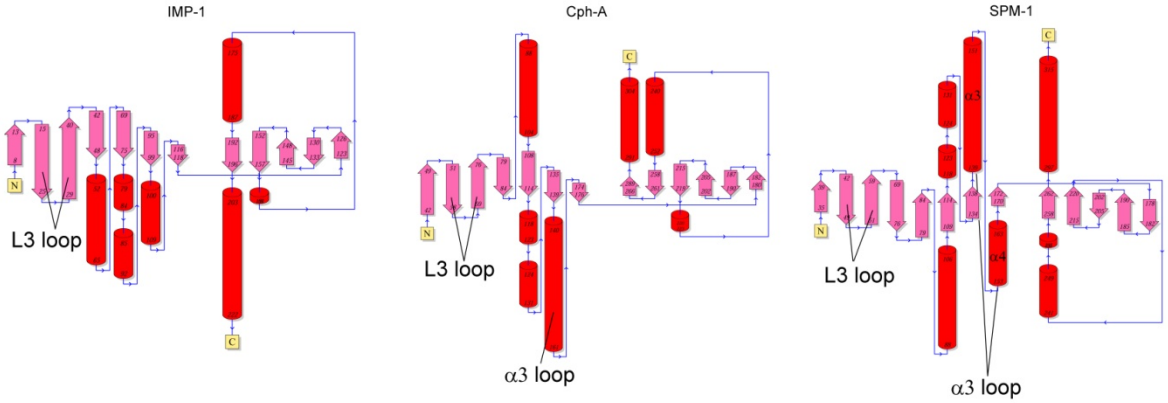

Figure. S5. Purification of di-Zn(II)-SPM-1. A – FPLC chromatogram and SDS-PAGE analysis of fractions from the HisTrap HP column (Ni-NTA resin); B – di-Zn(II)-SPM-1 after His-tag cleavage M = molecular weight markers (PageRuler Prestained Protein Ladder 10-170 kDa, Thermo Scientific), lane 1 - before the cleavage with 3C protease; lane 2 mixture of the cleaved and uncleaved enzyme; lane 3 after cleavage with 3C protease.

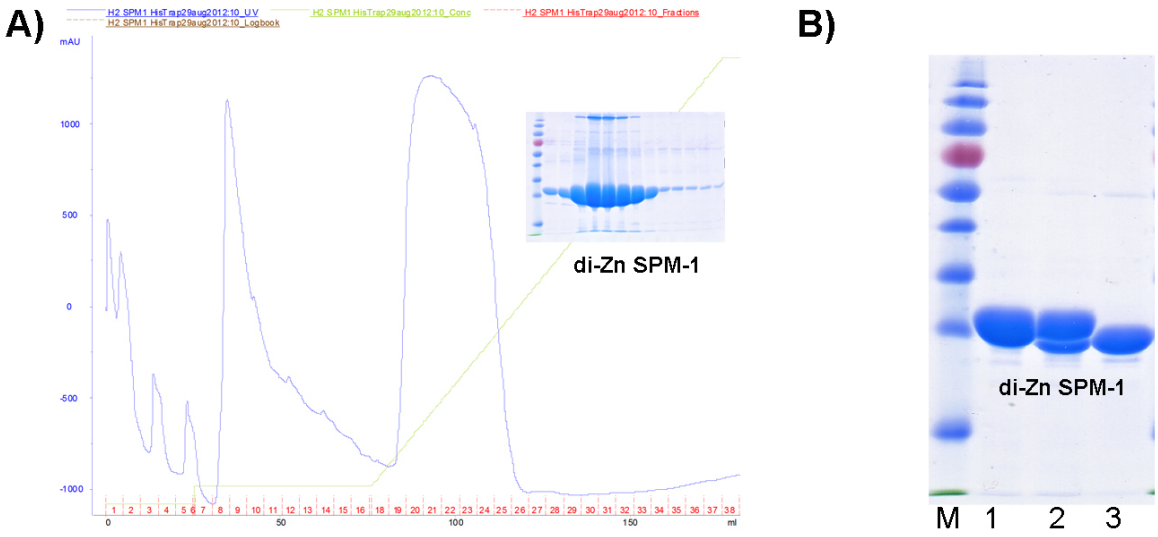

Figure S6. Production of apo SPM-1. FPLC chromatogram and SDS-page gel of fractions from the gel filtration column (Superdex S200, 300mL).

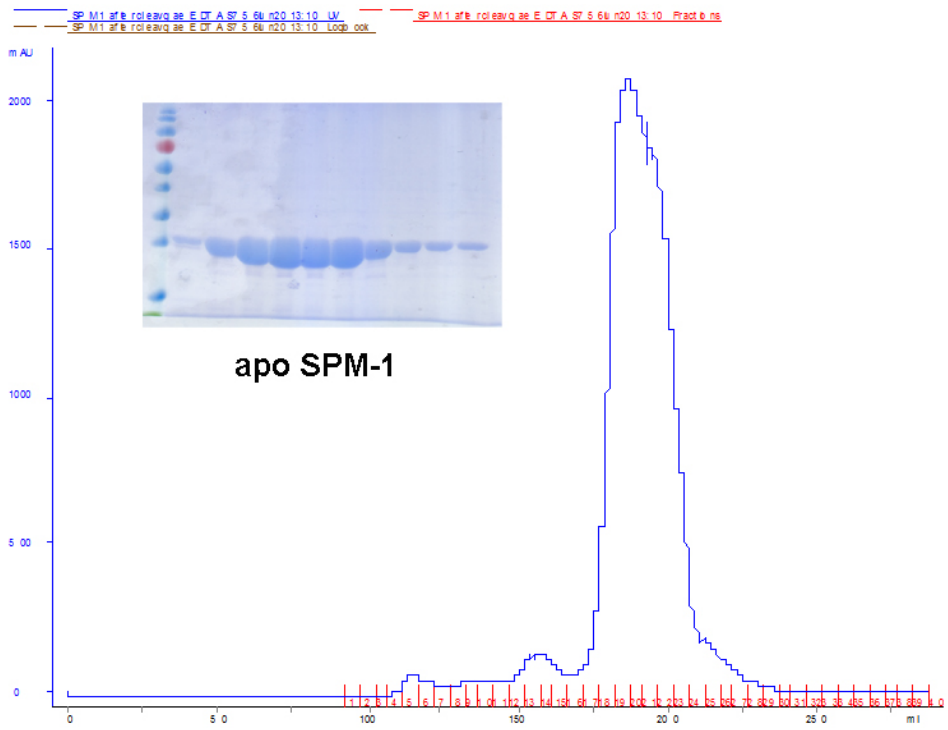

Figure S7. MS spectra of SPM-1 variants. A) Denatured MS spectra of SPM-1. The observed mass (27887 Da) by LC MS is consistent with the predicted mass (27884 Da) of SPM-1; B) MS spectra of apo-SPM-1. Note: Apo-enzyme was obtained by treatment with EDTA of the di-Zn(II)-SPM-1 (see protein preparation); C) MS spectra of di-Zn(II)-SPM-1. Non-denaturing ESI-MS of SPM-1 at a cone voltage of 50V. The observed mass difference (+120) with the apo-protein corresponds to the di-Zn MS form of SPM-1.

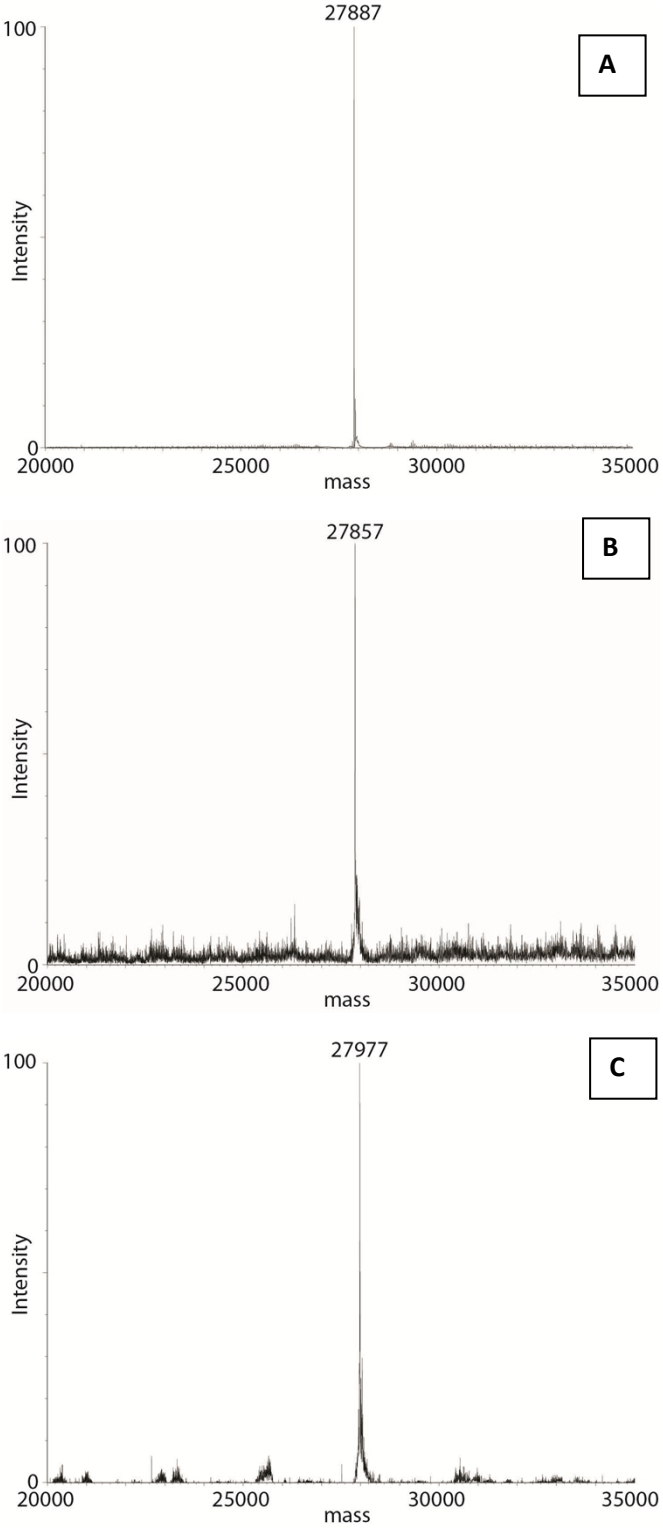

Figure S8. Thermal shift results with SPM-1 using different metals and buffers. A) Melting curves in HEPES and Tris buffer without added metal, an in the presence of Zn(II), Mn(II), Co(II) or Ni(II) (50 µM final concentration) in HEPES buffer were measured. B) Data represent the mean of triplicate experiments, with error bars showing the standard error of the mean (±SEM).

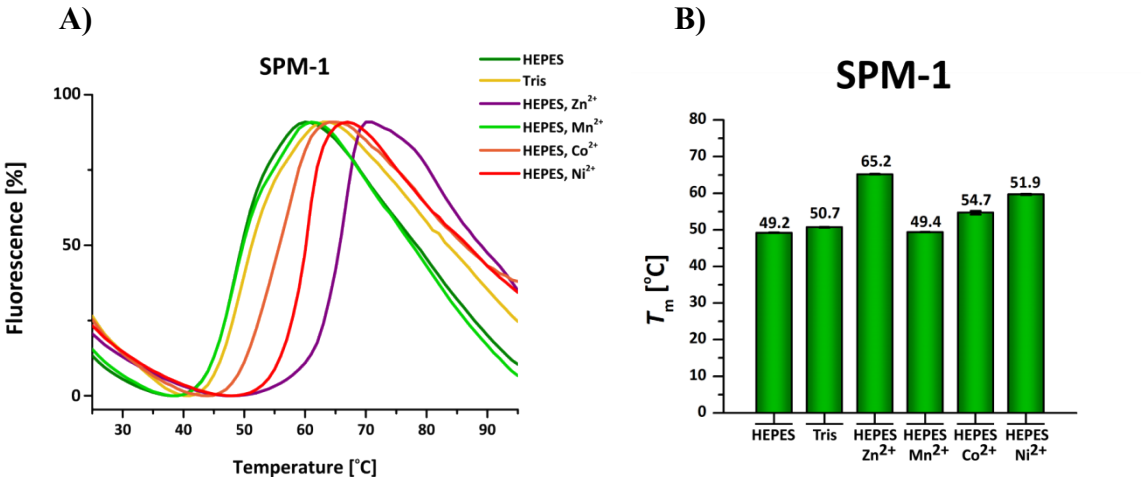

Table S2. Data collection and refinement statistics.

	SPM-1
Data collection	
Space group	$P\,2_1\,2_1\,2_1$
Unit cell dimensions	
a,b,c (Å)	45.65 83.55 282.41
α,β,γ (°)	90,90,90
Resolution (Å) (outer shell)	71.91-2.24 (2.32-2.24)
No. of molecules/ASU	4
No. of unique reflections	53264
Completeness (%)	99.89 (99.98)
Redundancy	6.4
R_{merge}	0.08
Mean I/σ(I)	14.09 (2.84)
Wilson B value (Å^2)	40.96
Refinement	
R_{factor}	0.1616 (0.2517)
R_{free}	0.2041 (0.2973)
R.m.s.d.	
Bond length (Å)	0.009
Bond angle (°)	1.17
No. of atoms	8190
Protein	7707
Ligand/ion	65
Water	418
$<B_{factor}>$ (Å^2)	
Protein	49.50
Ligand/ion	67.30
Water	47.40

Numbers in parentheses refer to the highest resolution shell.
R_{merge} is the unweighted R-value on I between merged reflections.
$R_{factor} = \Sigma hkl \mid |F_{obs}(hkl)| - k|F_{calc}(hkl)| \mid / \Sigma hkl |F_{obs}(hkl)|$ for the working set of reflections; R_{free} is the R-value for 3.8% of the reflections excluded from refinement.

Figure S9. Collision cross sections of di-Zn(II)-SPM-1, apo-SPM-1 and the di-Zn(II)-IMP-1 as determined by IM MS.

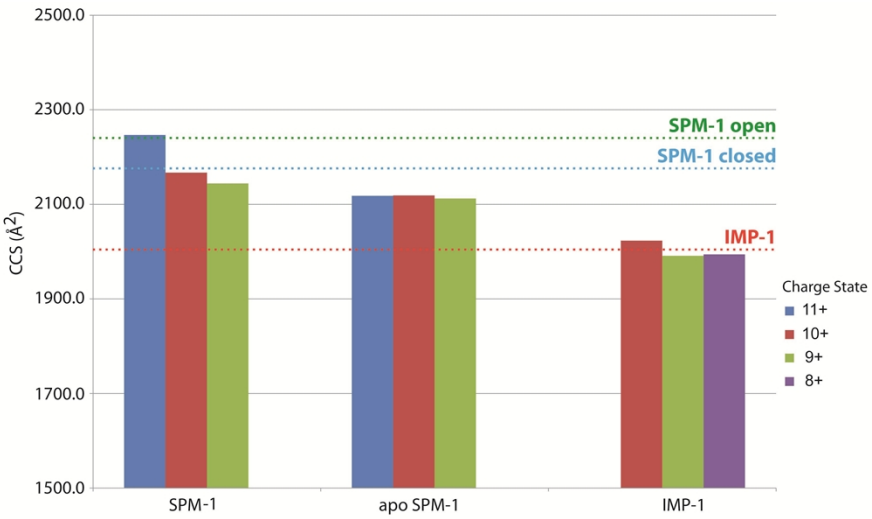

Figure S10. Positions of the SPM-1 Y152C substitutions (in red) modelled using the 'open' (PDB: 2FHX) and 'closed' (PDB 4BP0) structures of SPM-1.

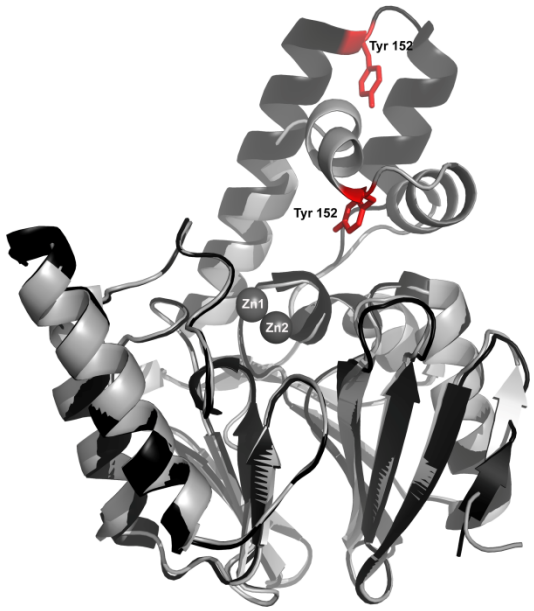

Figure S11. Expression trial for di-Zn(II)-Y152C SPM-1. SDS-PAGE analysis for the expression trials of Y152C;gels shows M = molecular weight markers (PageRuler Prestained Protein Ladder 10-170 kDa, Thermo Scientific), lane 1 - uninduce sample, lane 2 - 37 °C/4h, lane 3 - 37 °C/20h, lane 4 - 30 °C/4h, lane 5 - 30 °C/20h, lane 6 - 18 °C/4h and lane 7 - 18 °C/20h.

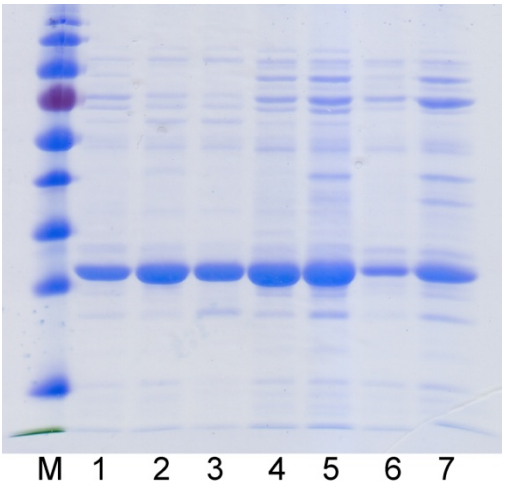

Figure S12. Purification of di-Zn(II)-Y152C SPM-1. A – FPLC chromatogram and SDS-PAGE analysis of the HisTrap HP column (Ni-NTA resin); B – di-Zn SPM-1 after His-tag cleavage; M = molecular weight markers (PageRuler Prestained Protein Ladder 10-170 kDa, Thermo Scientific), lane 1 - and 2 di-Zn(II)-Y152 SPM-1 mutant after His-tag cleavage.

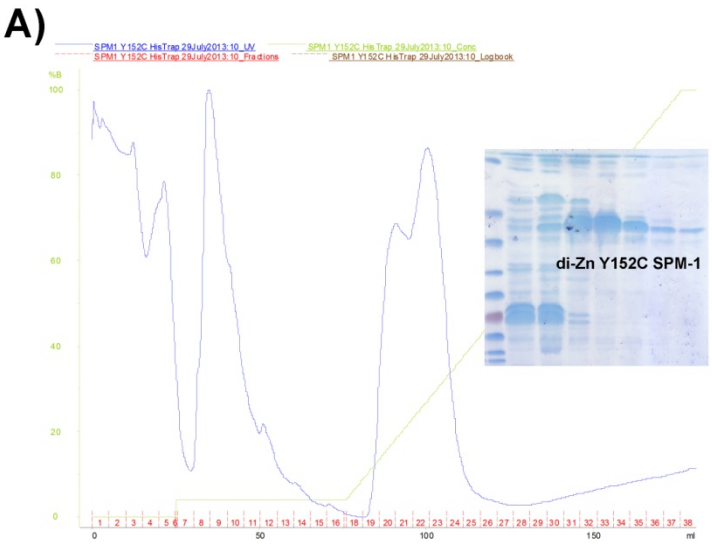

Figure S13. MS spectra of SPM-1 Y152C and SPM-1 Y152C labelled with 3-bromo-1,1,1-trifluoro acetone (SPM-1*). The observed mass of SPM-1 Y152C (27824.1) corresponds with the predicted mass (27827). The observed mass difference (+129) for the labelled enzyme corresponds to attachment of one 1,1,1-trifluoro acetone (BFA) label per SPM-1 Y152C.

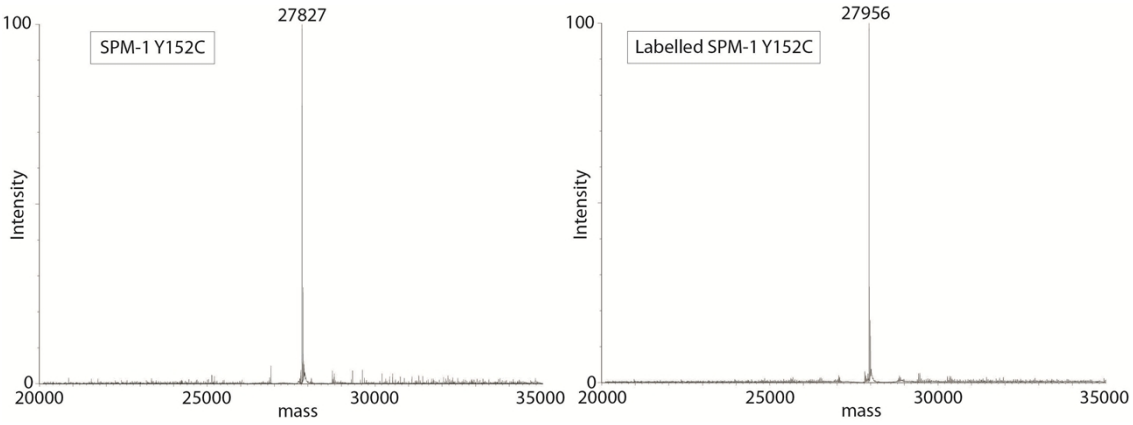

Figure S14. MALDI-TOF MS spectra of SPM-1 Y152C and SPM-1*. MALDI-TOF MS spectra of labelled and unlabelled SPM-1 Y152C digested with trypsin. Free cysteines in the samples were reduced and *S*-carbamidomethylated (Cys^{CAM}) prior to digestion. A) complete spectrum of the digested sample is shows; B) close-up of the assigned modified peptide (labelled: m/z = 1020.4, *S*-carbamidomethylated: m/z 965.4); C) MALDI-ToF-ToF fragmentation of a labelled precursor $[IKAAEF\underline{C}K+H]^+$ (m/z = 1020.4) from trypsin digestion of the BFA-labelled SPM-1 mutant Y152C. The data support modification of C152. Ions coloured in red are modified by the label; black coloured ions are unlabelled.

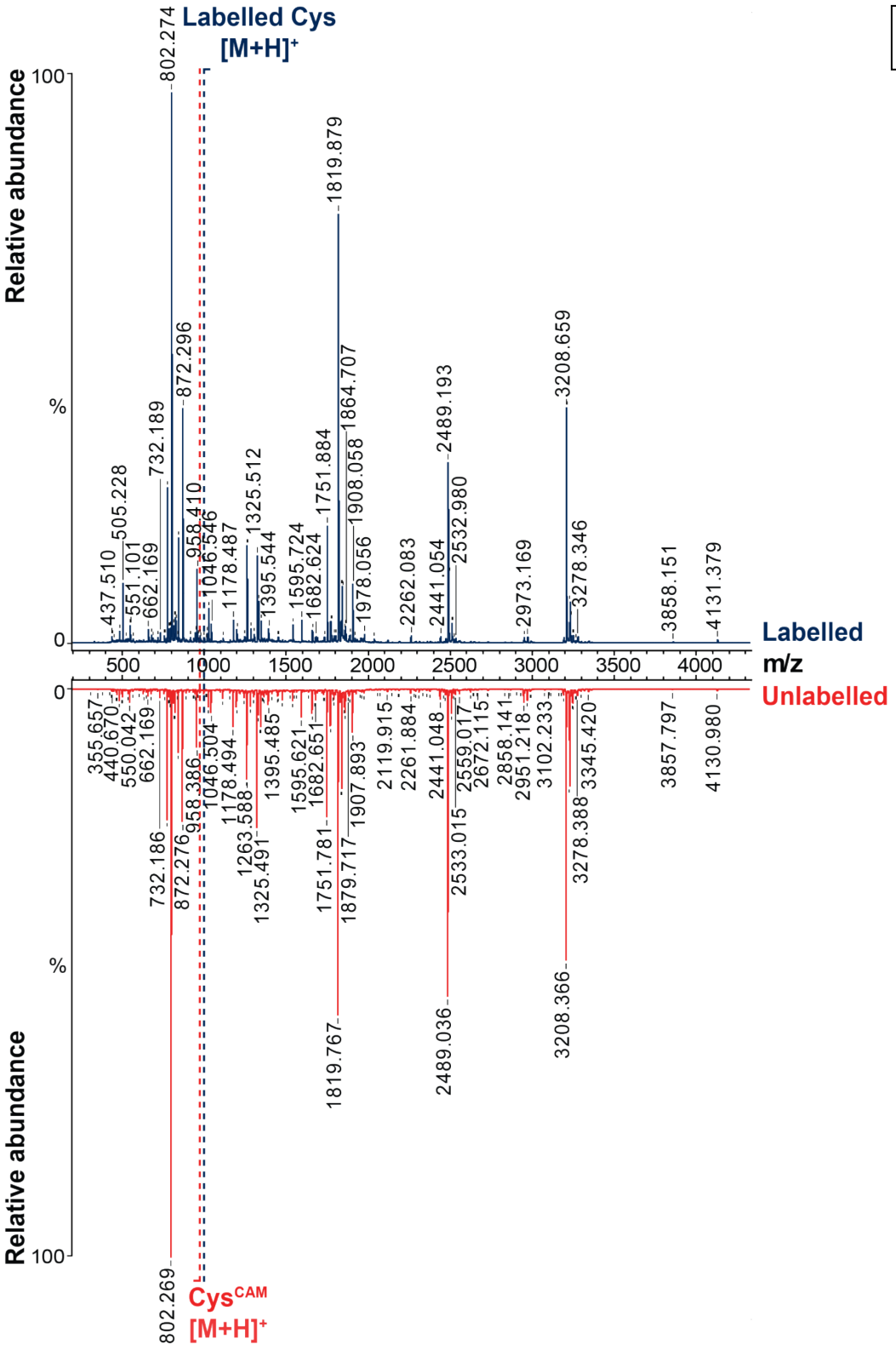
A
Labelled Cys
[M+H]+
Relative abundance
100
%
0
802.274
872.296
732.189
505.228
437.510
662.169
551.101
958.410
1046.546
1178.487
1325.512
1395.544
1595.724
1682.624
1751.884
1908.058
1864.707
1819.879
1978.056
2262.083
2441.054
2489.193
2532.980
2973.169
3208.659
3278.346
3858.151
4131.379
500
1000
1500
2000
2500
3000
3500
4000
m/z
Labelled
Unlabelled
0
%
100
Relative abundance
802.269
Cys^CAM
[M+H]+
355.657
440.670
550.042
662.169
732.186
872.276
958.386
1046.504
1178.494
1263.588
1325.491
1395.485
1595.621
1682.651
1751.781
1819.767
1879.717
1907.893
2119.915
2261.884
2441.048
2489.036
2533.015
2559.017
2672.115
2858.141
2951.218
3102.233
3208.366
3278.388
3345.420
3857.797
4130.980

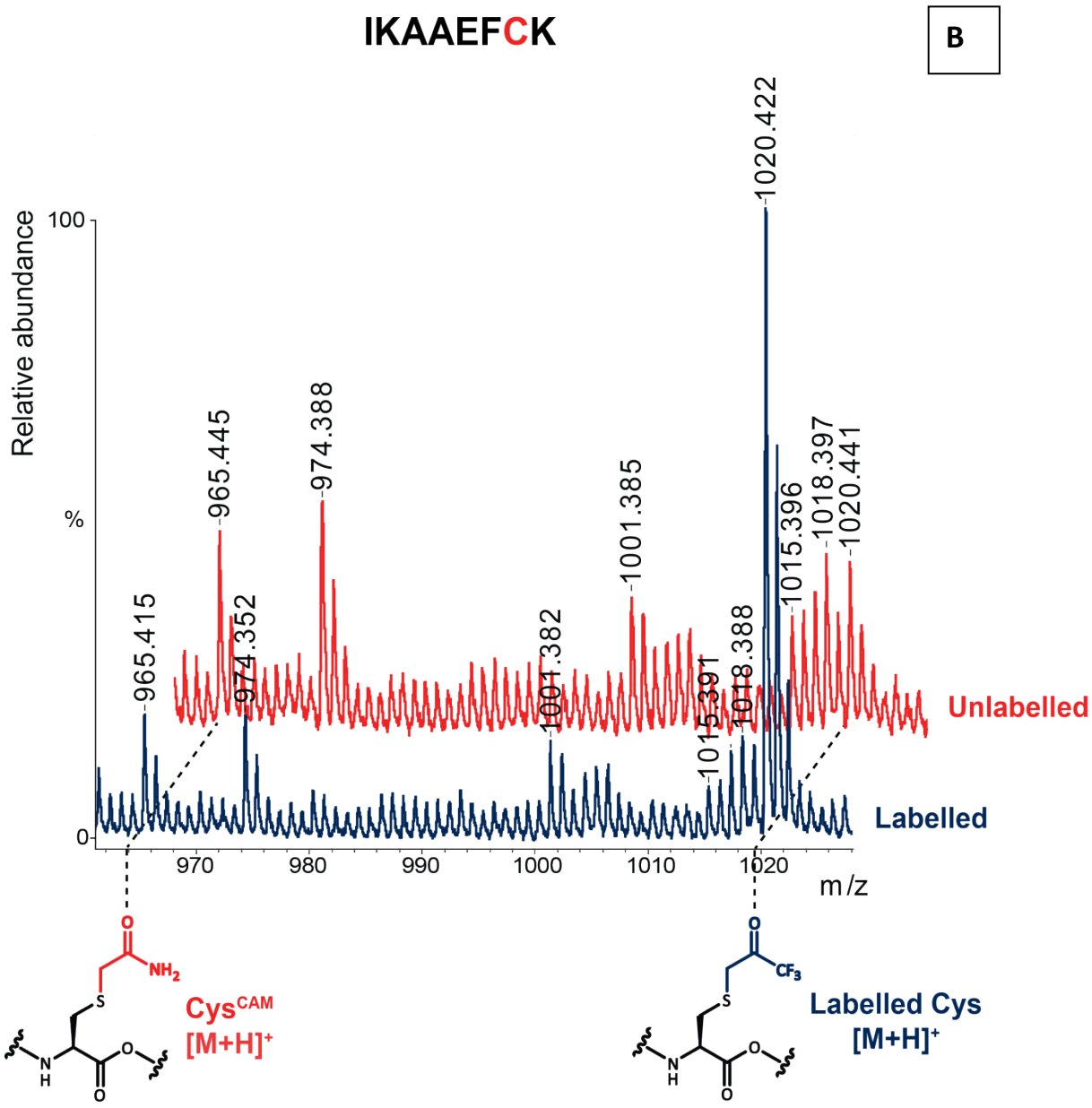
IKAAEFCK
B
Relative abundance
100
%
0
965.445
974.388
1001.385
1020.422
1018.397
1020.441
1015.396
965.415
974.352
1001.382
1015.391
1018.388
Unlabelled
Labelled
970
980
990
1000
1010
1020
m/z
Cys^CAM
[M+H]+
Labelled Cys
[M+H]+

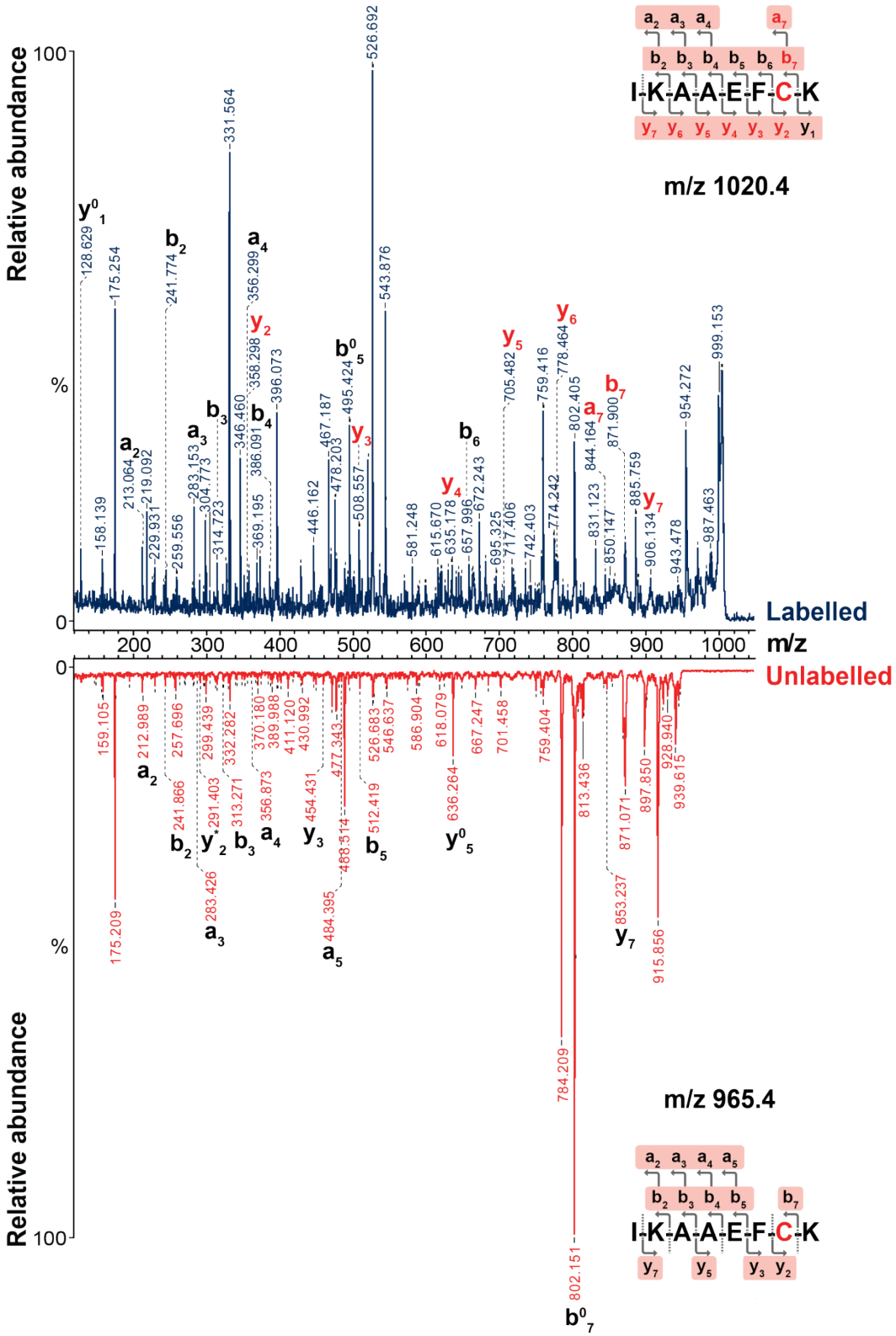
Relative abundance
100
%
0
Labelled
m/z
Unlabelled
200
300
400
500
600
700
800
900
1000
m/z 1020.4
m/z 965.4
I-K-A-A-E-F-C-K
Relative abundance
100
%
0

Figure S15. Comparison of ^{19}F NMR spectra of different ^{19}F labelled MBLs. (From top to bottom): denatured NDM-1*, denatured SPM-1,* and non-denatured SPM-1*. Denaturation of SPM-1* by treatment with 2M guanidine HCl solution (12 hours) leads to a signal broadening as observed for the denatured NDM-1* sample.[8]

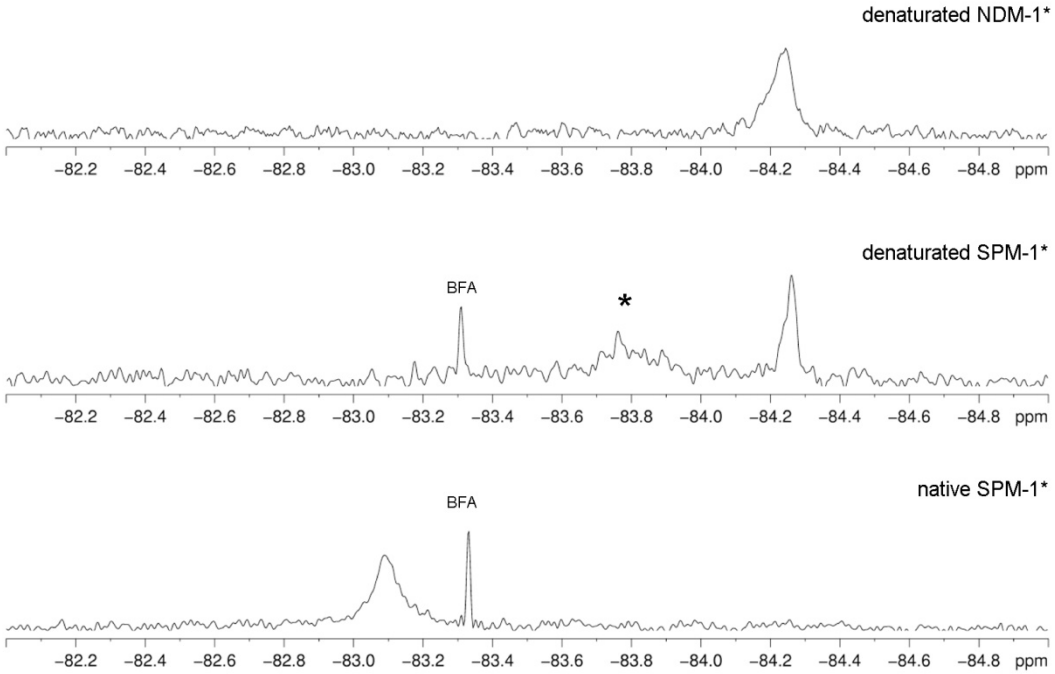

* Possible intermediate.

Figure S16. Time course analyses of SPM-1* treatment with EDTA followed by ^{19}F NMR. Note that the sequestration of metal from the di-Zn(II)-SPM-1* complex with 5 mM EDTA is rapid.

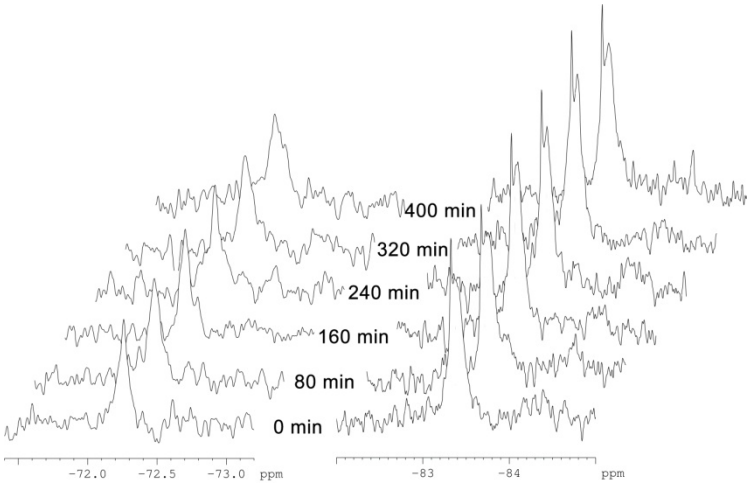

Figure S17. Comparison of the ^{19}F NMR spectra of di-Zn(II) and apo-SPM-1*.

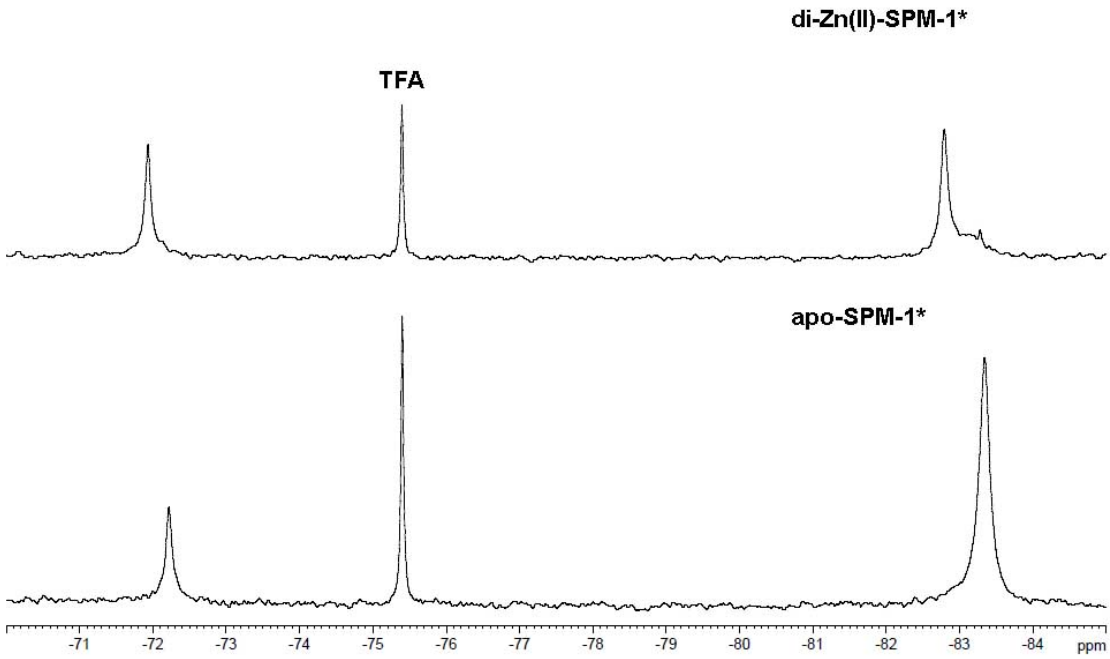

Figure S18. Solvent exposure experiments on ^{19}F-labelled SPM-1. The change in chemical shift for the shielded signal shift (δ = -83 ppm) of di-Zn(II)-SPM-1*, was fitted with a linear function gives y=0.00087x, R^2>0.99; this corresponds to 58% exposure.[8] The change in chemical shift for the deshielded signal shift (δ = -72 ppm) of di-Zn(II)-SPM-1*, fitted with a linear functions gives y=0.00149x, R^2>0.99; corresponding to 99% solvent exposure. The percentage solvent exposures of SPM-1* label (shielded signal shift) were calculated as a ratio of the slope obtained for the SPM-1* complex relative to the analogous slope for TFA in the sample (set to 100% as a fully exposed small molecule signal).[8]

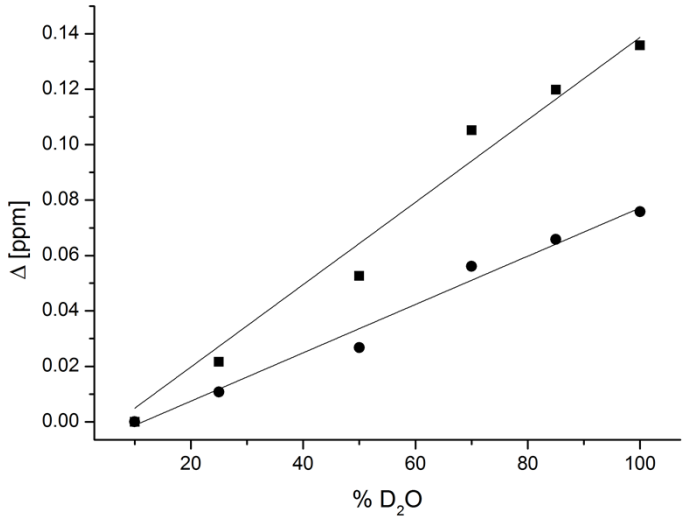

Figure S19. Saturation transfer experiment for the di-Zn(II)-SPM-1* using ^{19}F NMR.

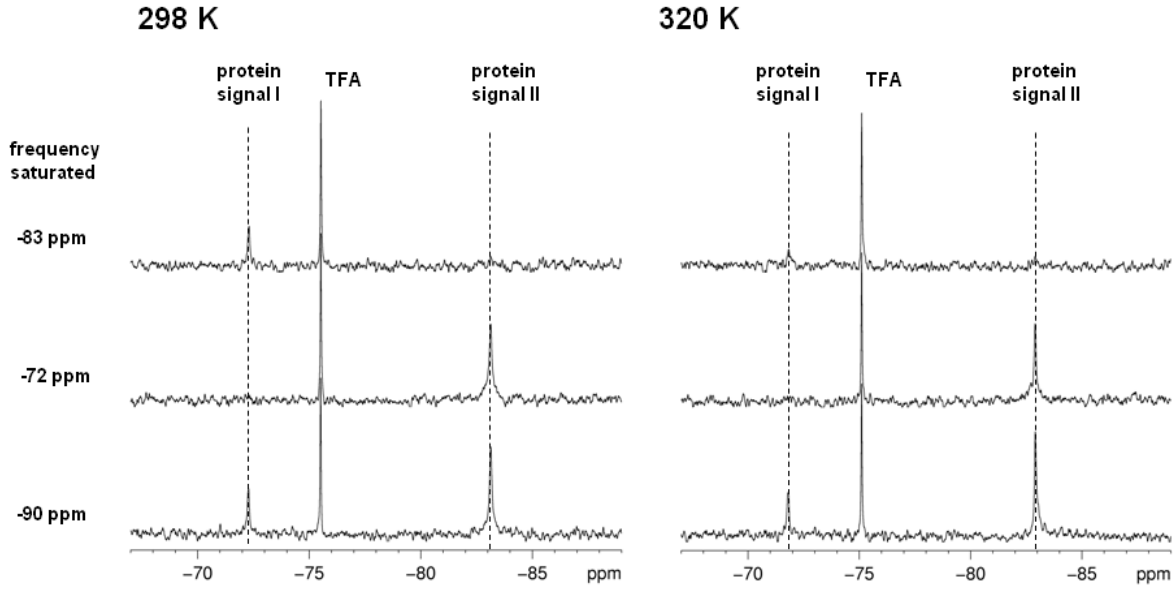

Table S3. Summary of results from saturation transfer experiment results.

Temp. [K]	decrease in -72 ppm peak intensity when -83 ppm peak saturated	decrease in -83 ppm peak intensity when -72 ppm peak saturated	ratio of peak intensities (-72/-83 ppm)
298	28%	5%	1:2
320	70%	25%	1:4

Table S4. Experimental and CIFIT calculated data for the selective magnetisation transfer experiment (Peak A = -82.2 ppm, Peak B= -71.4 ppm).

Time /s	*Calc A*	*Calc B*	*Expt A*	*Expt B*
0.001	1.3476	-0.9926	1.3488	-1
0.04	1.2996	-0.7569	1.3203	-0.7838
0.08	1.2649	-0.5432	1.3308	-0.5842
0.1	1.2522	-0.4458	1.2337	-0.4587
0.15	1.2316	-0.227	1.2337	-0.1614
0.2	1.2238	-0.039	1.2249	-0.0168
0.25	1.2256	0.123	1.1913	0.1123
0.3	1.2343	0.2627	1.2162	0.3111
0.35	1.2481	0.3836	1.242	0.3467
0.4	1.2654	0.4883	1.2459	0.4696
0.45	1.2849	0.5793	1.2715	0.5586
0.5	1.3056	0.6584	1.3773	0.6434
0.7	1.3898	0.8864	1.3825	0.8927
0.9	1.4618	1.0215	1.465	1.0513
1.8	1.6083	1.2135	1.5877	1.1834
3	1.6356	1.2408	1.6383	1.2432

Figure S20. ^{19}F NMR spectra of the di-Zn(II)-SPM-1 with 3,5-bis(mercaptomethyl)benzoic acid. Note that broadening of both fluorine signals ('open' conformation at -72 ppm and the 'closed' conformation at -83 ppm) was observed upon the addition of 1 mM 3,5-bis(mercaptomethyl)benzoic acid (top spectra) suggesting that the inhibitor binds to the active site of SPM-1 (bottom spectra di-Zn SPM-1*).

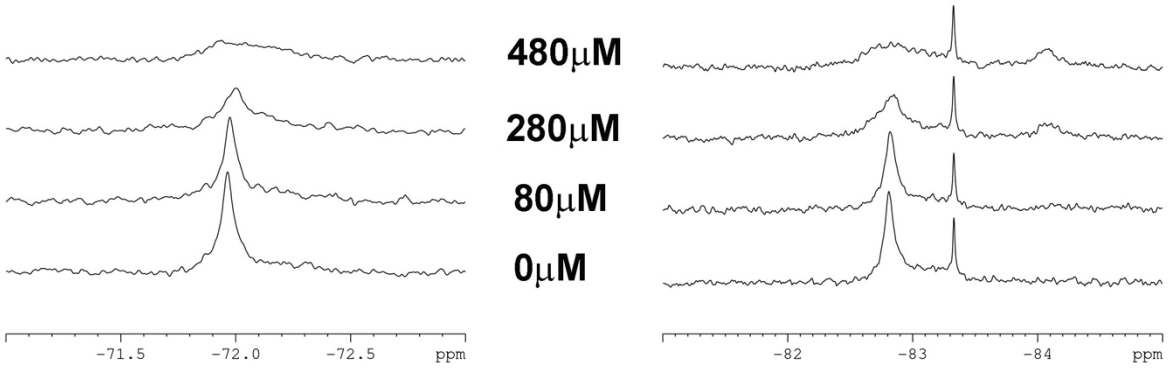

Figure S21. ^{19}F NMR spectra the di-Zn(II)-SPM-1* with thiosalicylic acid. Note that both fluorine signals change and slightly broaden ('open' conformation at δ - 72 ppm and the 'closed' conformation at δ - 83 ppm) was observed upon the addition of 1 mM thosalicylic acid (top spectra) suggesting thiosalicylic acid bind to the active site of SPM-1 (bottom spectra di-Zn SPM-1*). Both 3,5-bis(mercaptomethyl)benzoic acid and thosalicylic acid are thiols; interestingly for 3,5-bis(mercaptomethyl)benzoic acid the line broadening characteristic of fast exchange systems is more pronounced compared to thiosalicylic acid (it appears thiosalicylic acid-di-Zn(II)-SPM-1* complex remains a slow exchange system) suggesting the two thiols bind in different modes.

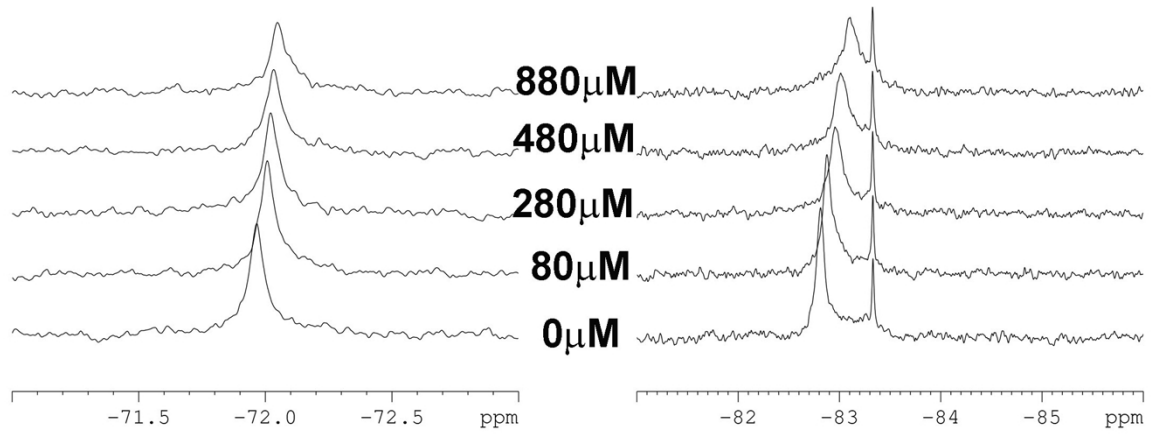

Figure S22. Zinc dependence of SPM-1 catalysed hydrolysis of FC5 ((6*R*,7*R*)-8-oxo-3-(((2-oxo-2*H*-chromen-7-yl)oxy)methyl)-7-(2-phenylacetamido)-5-thia-1-azabicyclo[4.2.0]oct-2-ene-2-carboxylic acid 5,5-dioxide; 2.5 μM). Note the increase of the activity of SPM-1 (0.5 nM) by using a higher concentration of zinc; this is characteristic for B1, but not for B2, MBLs (B2 MBLs are typically inhibited by an excess of Zn(II)).[17] Note also that the apparent non-levelling effect of zinc likely reflects the observation that at higher Zn concentrations protein precipitation was observed.

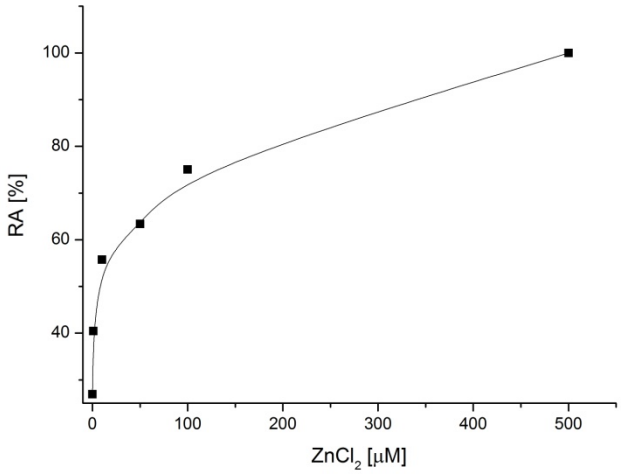

Figure S23. Stopped-flow analysis of the hydrolysis of meropenem by SPM-1-Co(II). Reactions were conducted at 5 °C and monitored using a photodiode array detector. SPM-1 (100 μM) was incubated with Co(II) (500 μM) for ~10 min, then mixed with meropenem (100 μM) in an 1:1 ratio. A-D – time-resolved absorbance spectra; F-H – Spectra whereby the first trace of a defined time interval was subtracted.

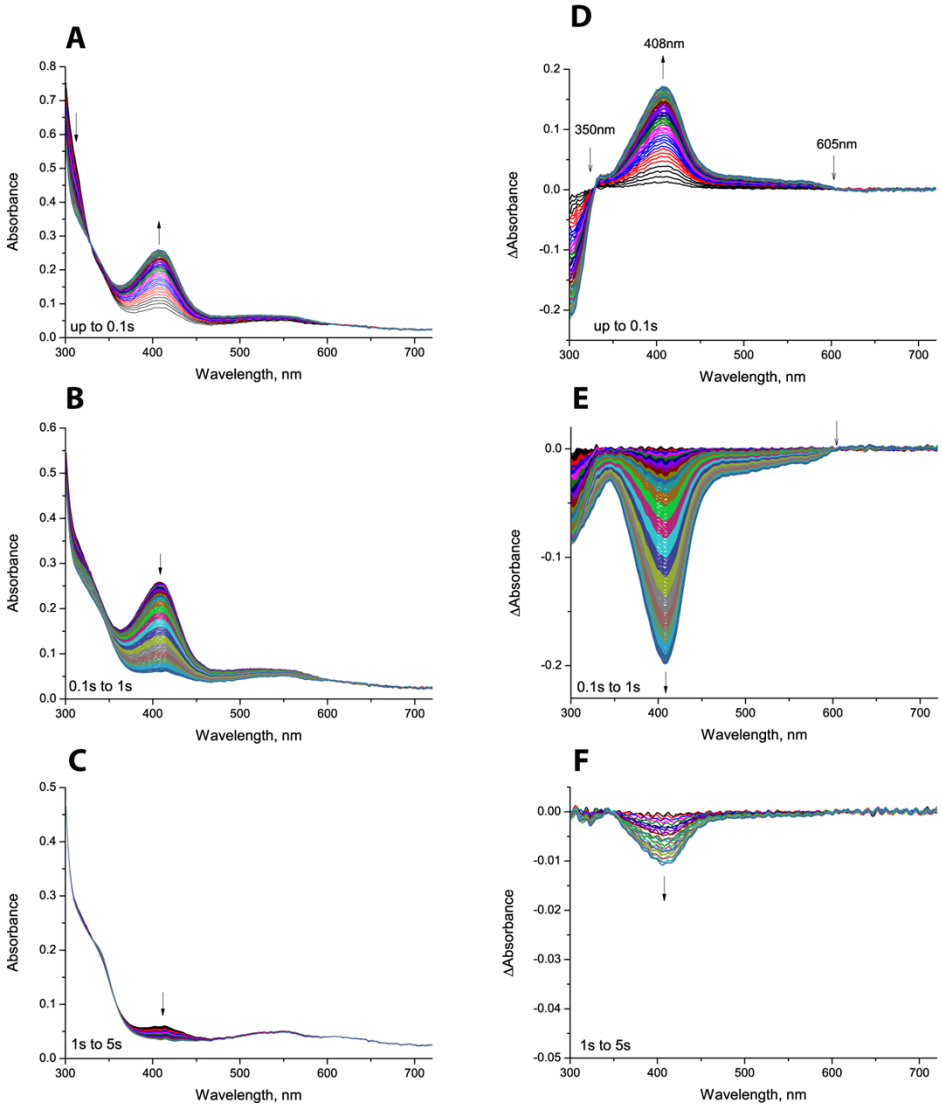

Figure S24. Stopped-flow time course of the hydrolysis of meropenem by SPM-1-Co(II). A-D – time-resolved absorbance spectra. Note, we also studied the reaction of SPM-1 which was substituted with different SPM-1/Co(II) ratios. The level of intermediate accumulation, and the hydrolysis were found to be dependent on the Co(II) concentration, with no other species being spectroscopically observed at lower Co(II) concentration (Fig. 4A). Increasing Co(II) up to 5 equivalents (compared to apo-SPM-1) did not result in significant changes of the kinetics compared to a 1:2 SPM-1:Co(II) ratio (Fig. 25B).

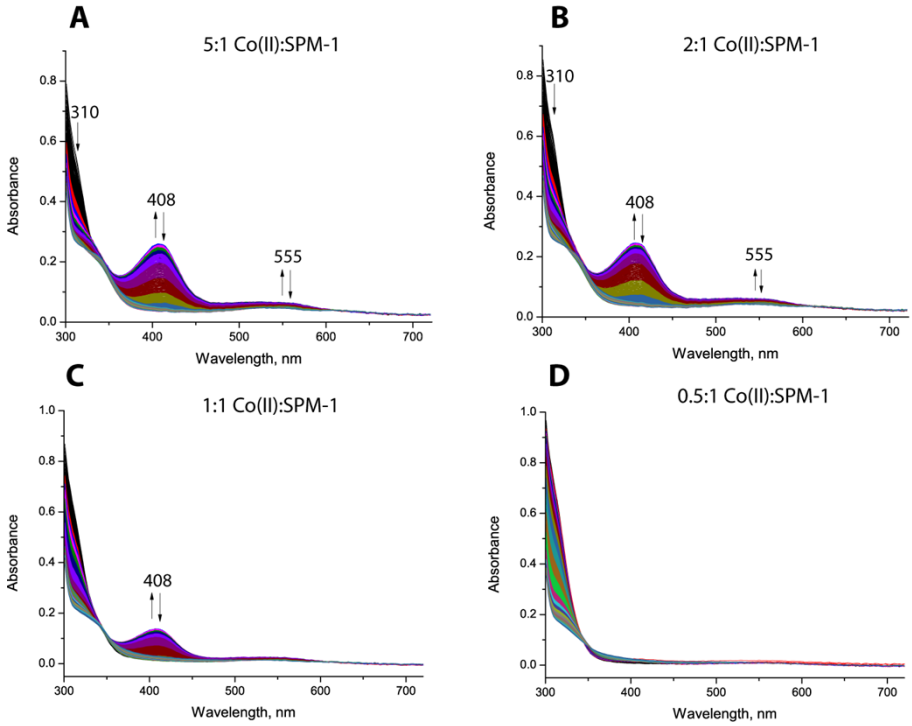

Figure S25. Fit to Model 1. This model considers only the reaction of di-Co(II)-SPM-1 (E).

The single wavelength absorption traces were analysed, and a global fit was performed in order to propose a minimal kinetic mechanism. In view of the proposed difference in the affinity of Zn1 and Zn2 binding for SPM-1 and lack of information on Co(II) binding constants[18] (an attempt to take Co(II) binding into account resulted in a poor fit, see Model 2 below), the data obtained using a 1:5 SPM-1:Co(II) ratio were analysed assuming only di-Co(II) SPM-1 was present in solution prior to reaction. The best fit was obtained using the mechanism shown in Fig.3C. Consistent with BcII-Co(II), the proposed mechanism suggests formation of ES, EI1 (408 nm band) and EI2 (an intermediate with localization of the negative charge on C-3 of the substrate (555 nm band)) complexes (see Figure. S24); however, the EI2 complex is likely to be unproductive and to exist in equilibrium with the EI1 intermediate. Thus, observation of similar absorbance species to that

observed for BcII in the catalysis by SPM-1 suggests that SPM-1 employs a mechanism similar to that proposed for BcII and other B1 MBLs.

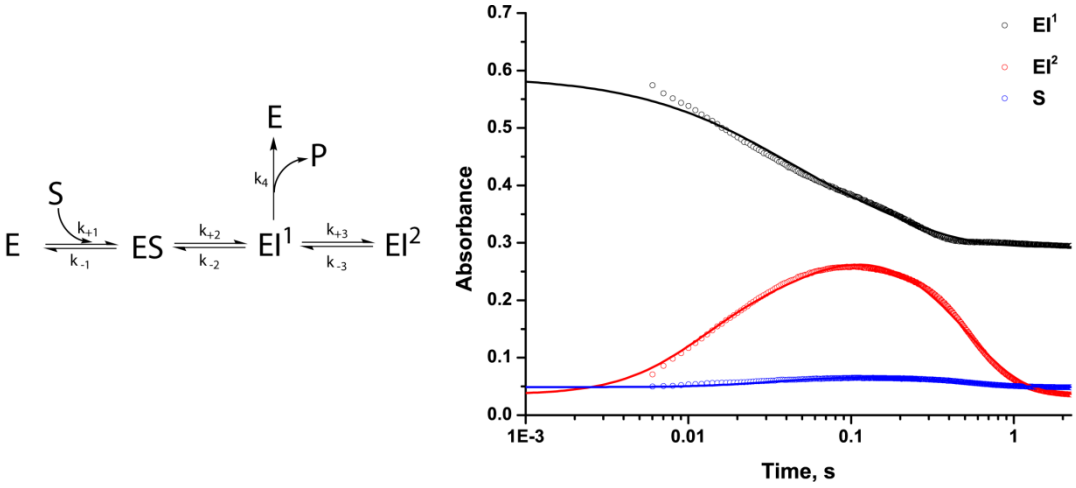

Table S5. Parameters used for simulation of the reaction kinetics for the hydrolysis of meropenem by Co(II)-substituted SPM-1. Conditions: 50 µM SPM-1 (incubated with 250 µM Co(II)) reacted with 50 µM meropenem. The model considers SPM-1 as a di-Co(II) species.

	best fit parameter	relative error, %
$k_{+1}(\mu M^{-1}*s^{-1})$	0.617	5.4
$k_{-1}(s^{-1})$	47.6	24.0
$k_{+2}(s^{-1})$	233.8	10.5
$k_{-2}(s^{-1})$	26.1	26
$k_3(s^{-1})$	60.4	7.2
$k_{-3}(s^{-1})$	69.7	7.0
$k_4(s^{-1})$	6.08	0.4
$r_S(M^{-1}*cm^{-1})$	5928	4.9
$r_{EI1}(M^{-1}*cm^{-1})$	1591	23
$r_{EI2}(M^{-1}*cm^{-1})$	1331	1.5

Figure S26 Fit to Model 2. This model considers reaction of di-Co(II)-SPM-1 (E) taking into account different binding affinities of Co(II) for apo-SPM-1 and mono-substituted Co(II)-SPM-1 (1:1 SPM-1:Co(II) ratio).

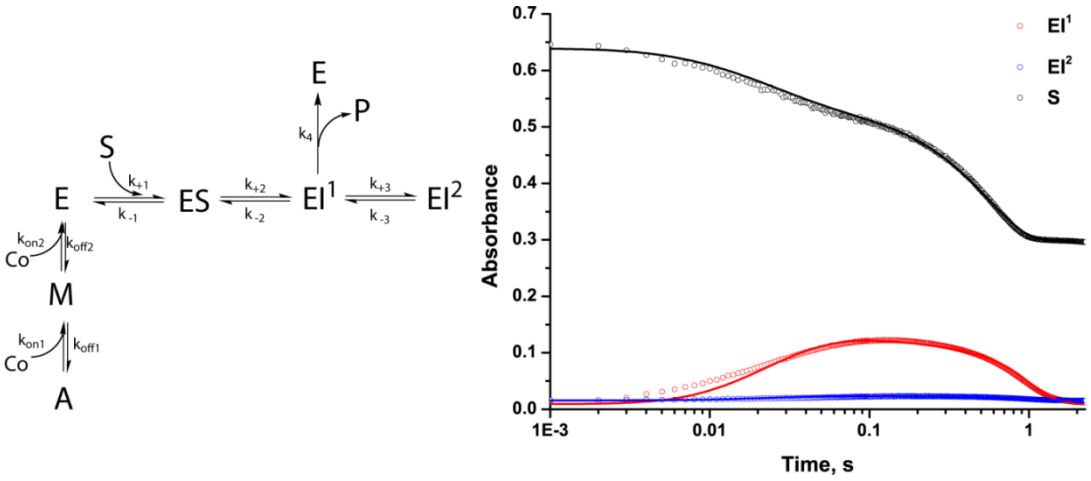

Table.S6. Parameters used for simulation of the reaction kinetics of Co(II)-substituted SPM-1 with meropenem. Conditions: 50 µM SPM-1 (incubated with 50 µM Co(II)) reacted with 50 µM meropenem. Due to the lack of the information regarding the binding constants of Co(II) to SPM-1, k_{on1}, k_{off1}, k_{on2}, k_{off2} were allowed to 'float' in the first rounds of the simulations, which after these parameters were fixed.

	best fit parameter	relative error, %
$k_{on1}(\mu M^{-1}*s^{-1})$	1.2	fixed
$k_{off1}(s^{-1})$	2.02	fixed
$k_{on2}(\mu M^{-1}*s^{-1})$	12.2	fixed
$k_{off2}(s^{-1})$	1300	fixed
$k_{+1}(\mu M^{-1}*s^{-1})$	8.79	98
$k_{-1}(s^{-1})$	255	119
$k_{+2}(s^{-1})$	282	68
$k_{-2}(s^{-1})$	74.8	105
$k_3(s^{-1})$	103000	29.5
$k_{-3}(s^{-1})$	1520	67.5
$k_4(s^{-1})$	309	120
$r_S(M^{-1}*cm^{-1})$	68210	ND
$r_{EI1}(M^{-1}*cm^{-1})$	1583	50
$r_{EI2}(M^{-1}*cm^{-1})$	542	1.5

References

1. S. S. van Berkel, J. Brem, A. M. Rydzik, R. Salimraj, R. Cain, A. Verma, R. J. Owens, C. W. G. Fishwick, J. Spencer and C. J. Schofield, *J. Med. Chem.*, 2013, **56**, 6945-6953.
2. Z. Otwinowski and W. Minor, Elsevier, 1997, vol. **276**, pp. 307-326.
3. A. J. McCoy, R. W. Grosse-Kunstleve, P. D. Adams, M. D. Winn, L. C. Storoni and R. J. Read, *J. Appl. Crystallogr.*, 2007, **40**, 658-674.
4. T. A. Murphy, L. E. Catto, S. E. Halford, A. T. Hadfield, W. Minor, T. R. Walsh and J. Spencer, *J Mol Biol*, 2006, **357**, 890-903.
5. P. D. Adams, P. V. Afonine, G. Bunkoczi, V. B. Chen, I. W. Davis, N. Echols, J. J. Headd, L. W. Hung, G. J. Kapral, R. W. Grosse-Kunstleve, A. J. McCoy, N. W. Moriarty, R. Oeffner, R. J. Read, D. C. Richardson, J. S. Richardson, T. C. Terwilliger and P. H. Zwart, *Acta crystallogr., Sec. D: Biol. Crystallogr.*, 2010, **66**, 213-221.
6. P. Emsley, B. Lohkamp, W. G. Scott and K. Cowtan, *Acta crystallogr., Sec. D: Biol. Crystallogr.*, 2010, **66**, 486-501.
7. M. F. Bush, Z. Hall, K. Giles, J. Hoyes, C. V. Robinson and B. T. Ruotolo, *Anal. Chem.*, 2010, **82**, 9557-9565.
8. A. M. Rydzik, J. Brem, S. S. van Berkel, I. Pfeffer, A. Makena, T. D.W. Claridge and C. J. Schofield, *Angew. Chem., Int. Ed.*, 2014, **53**, 3129-3133.
9. A. D. Bain and J. A. Cramer, *J. Magn. Reson., Series A*, 1996, **118**, 21-27.
10. C. Bebrone, *Biochem. Pharmacol.*, 2007, **74**, 1686-1701.
11. K. Bush, *Ann. N.Y. Acad. Sci.*, 2013, **1277**, 84-90.
12. K. Bush and G. A. Jacoby, *Antimicrob. Agents Chemother.*, 2010, **54**, 969-976.
13. G. Cornaglia, H. Giamarellou and G. M. Rossolini, *The Lancet Infect. Dis.*, 2011, **11**, 381-393.
14. M. W. Crowder, J. Spencer and A. J. Vila, *Acc. Chem. Res.*, 2006, **39**, 721-728.
15. W. Fast and L. D. Sutton, *Biochim. Biophys. Acta*, 2013, **1834**, 1648-1659.
16. M. I. Page and A. Badarau, *Bioinorg. Chem. Appl.*, 2008, DOI: 10.1155/2008/576297, 576297.
17. A. I. Karsisiotis, C. F. Damblon and G. C. K. Roberts, *Metallomics*, 2014, DOI: 10.1039/C4MT00066H.
18. M. F. Tioni, L. I. Llarrull, A. A. Poeylaut-Palena, M. A. Marti, M. Saggu, G. R. Periyannan, E. G. Mata, B. Bennett, D. H. Murgida and A. J. Vila, *J. Am. Chem. Soc.*, 2008, **130**, 15852-15863.